Wakefield Induced Correlated Energy Spread and Emittance Growth at TTF FEL

Feng ZHOU*

DESY-MPY, Notkestr.85, 22603 Hamburg, Germany

Abstract

An electron beam with a small energy spread (0.1%) and a small normalized emittance (2 mm.mrad) is required to drive a Free Electron Laser at the TESLA Test Facility (TTF) at DESY. During FEL operations, the longitudinal and transverse wakefields which are generated by vacuum components, principally by RF cavities, bellows and valves, will induce an additional energy spread and emittance growth, respectively. This paper presents the wakefields and its induced correlated energy spread and emittance growth at the TTF FEL of phase I and II.

1 Introduction

The Free Electron Laser at the TESLA Test Facility (TTF FEL) is based on the principle of the so-called Self Amplified Spontaneous Emission (SASE) [1]. The goal is to obtain a coherent, very bright beam of photons with wavelengths tunable between 6 nm and 42 nm. This ambitious goal is realized by two steps [2], TTF FEL phase I and phase II, respectively. In phase I, a SASE FEL experiment will be firstly done at wavelength down to 42 nm by using 380 MeV TTF linac, as shown in Figure1(a). In phase II, 5 additional TESLA cryomodules are inserted and its energy is thus increased to 1.0 GeV with the wavelength down to 6 nm, as shown in Figure 1(b).

A small energy spread, a small transverse normalized emittance and high phase space densities in all three dimensions are mandatory for achieving micro bunching and saturation within an undulator of reasonable length. The longitudinal wakefield can increase the correlated energy spread, while the transverse wakefield can dilute the transverse emittance. In this paper we consider the short-range wakefields and its induced single bunch beam dynamics, correlated energy spread broadening and transverse emittance growth at the TTF Linac.

This paper is organized as follows: The second section is to present the short-range longitudinal wakefield of the vacuum components, such as cavities, bellows and valves, and their induced the energy spread broadening. In the third section, the short-range transverse wakefield and its induced emittance growth are estimated. The dispersion induced emittance growth is briefly discussed in the fourth section.

* On leave of absence from IHEP, Beijing

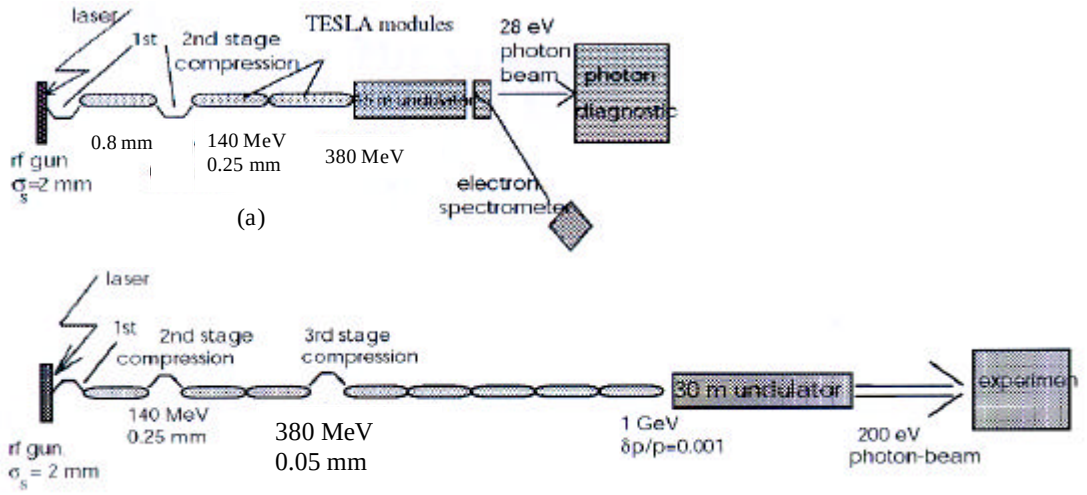

Figure 1: Layout of TTF FEL phase I and II

2 Correlated energy spread due to longitudinal wakefield

2.1 Longitudinal wakefield

TTF Linac contains vacuum components, such as RF cavities, bellows, valves and BPMs, which give rise to discontinuities in the beam pipe. As the beam traverses these discontinuities, the wakefield is then excited. The longitudinal wakefield of undulator beam pipe and its diagnostic section has been estimated [3]. The longitudinal wakefields of main vacuum components at TTF Linac except the undulator pipe and coherent effects in the bunch compressors, e.g, RF cavities, bellows and valves, are estimated in this section.

2.1.1 TESLA cavity

TESLA superconducting cavities are used to accelerator the beam in the TTF phase I and II. One cryomodule is composed of 8 cavities, one of which is composed of 9-cell cavity. As shown in Figure 1, the bunch length in the TTF Linac is shortened initially from 2 mm to 0.8 mm by the first stage bunch compression, from 0.8 mm to 0.25 mm, and finally from 0.25 mm to 0.05 mm by the second and third stage bunch compression, respectively. The longitudinal wakefield of cavities with different bunch length is calculated as follows.

a. Wakefield of 2 mm

At the exit of the RF gun the bunch is 2 mm long. Then, the bunch traverses the capture cavity which is composed of 9-cell cavity for the further acceleration and focusing after a longer drift. Due to its relative longer bunch length, the longitudinal wakefield of one cavity is easily calculated by MAFIA T2, as shown in Figure 2.

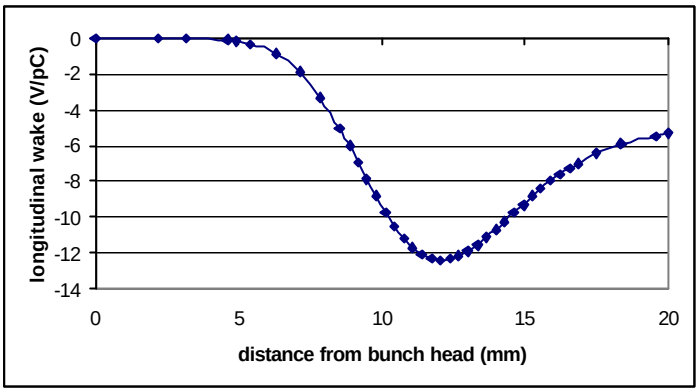

Figure 2: Longitudinal wakefield of one cavity with 2-mm-long bunch

b. Wakefield of 0.8 mm

Following the capture cavity, the first bunch compressor is used to compress the bunch length from 2 mm to 0.8 mm. Then, the bunch traverses the first cryomodule which includes eight 9-cell cavities. For a longer bunch, its total energy loss in multi-cavity structures would be then simply the sum of the losses in the individual cavities since the field pattern around the bunch is assumed unchanged before and after its travel through a cavity in the single-cavity approximation. However, this assumption is not valid for the short bunch smaller than 2 mm [5]. For short bunches, the field pattern changes tremendously after a passage through a cavity. For the bunch of 0.8 mm long, MAFIA calculations show that the wakefield of the third cavity is close to the convergence, which also agrees well with ABCI code calculations. Therefore, the wakefield of the following 5 cavities from #4 to #8 in one cryomodule is considered to be the wakefield of the third cavity. The wakefield of the cavity #1, 2 and 3 are shown in Figure 3.

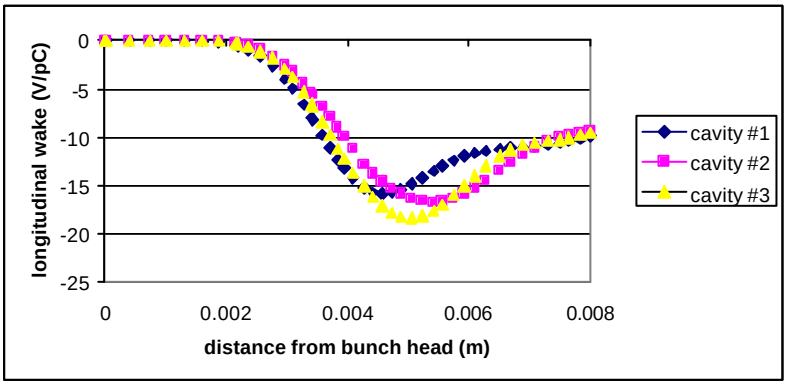

Figure 3: Longitudinal wakefield of the first 3 cavities
with the bunch length of 0.8 mm

c. Wakefield of 0.25 mm

After the second bunch compressor, the bunch is then shortened from 0.8 mm to 0.25 mm. It is understood that for such short bunch length one should calculate wakefield of the whole 8 cavities in one cryomodule in order to obtain its practical wakefield. However, it is a serious problem to use numerical codes to calculate the wakefield of 8 cavities of 8 m with such short bunch length. For such longer structures, the dispersion error due to the finite mesh size in the z direction need to be considered during the wakefield calculation for programmes as MAFIA, ABCI. The dispersion error can be suppressed effectively with the following condition:

$$\frac{\Delta z^2 \cdot L}{s_z^3} \le 1 \tag{1}$$

where L the total length of the structure, Δz the mesh size in the z direction, and s_z the bunch length. The mesh size in the z direction with different bunch length is given in Table 1.

Table 1: Mesh size in the z direction (unit: m m)

	L=1 m	8 m
s_z =0.8 (mm)	22.6	8
0.25	4.0	1.4
0.05	0.35	0.13

It is difficult to calculate the wakefield of 8 cavities due to its huge mesh points and unendurable long CPU time. For the case of the bunch length 0.25 mm, the wakefield of the first 3 cavities is computed by numerical method, as shown in Figure 4. The wakefield of the following 5 cavities are directly derived from the wake green function of the point charge, which is considered to be converged. The practical wakefield of the cavity from #4 to #8 is in between the wakefield of the third cavity and the converged one. However, since the energy spread induced by the wakefield of third cavity is close to the one of the converged wakefield, which will be compared in the next section, it is reasonable to estimate the wakefield of the cavity from #4 to #8 in one cryomodule to be the one from the wake green function. The wake green function of one TESLA cavity is expressed as [5]:

$$W_{11}^{\ d}(s) = 38.5(1.18 \times \exp(-0.577\sqrt{s}) - 0.18) \tag{2}$$

where s is the distance from the point charge. The wakefield of the bunch can be derived from the wake green function:

$$W_{11}(s) = \int r(s') \cdot W_{11}^{\ d}(s - s')ds' \tag{3}$$

where $W_{11}(s)$ is the wakefield of the bunch, $r(s)$ is the bunch distribution. The wakefield of the bunch with 0.25 mm from the green function is shown in Figure 5.

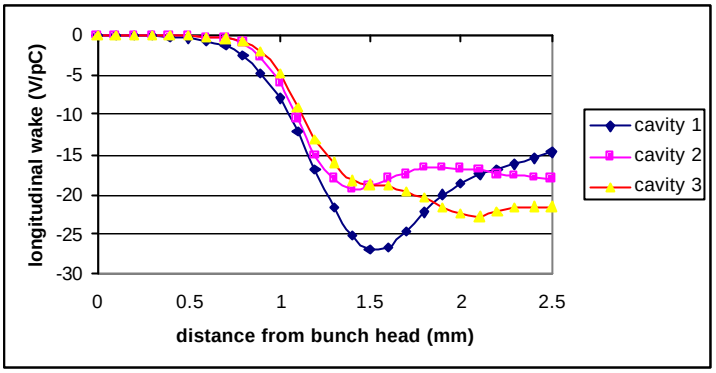

Figure 4: Longitudinal wakefield of cavity #1, 2 and 3 with 0.25-mm-long bunch

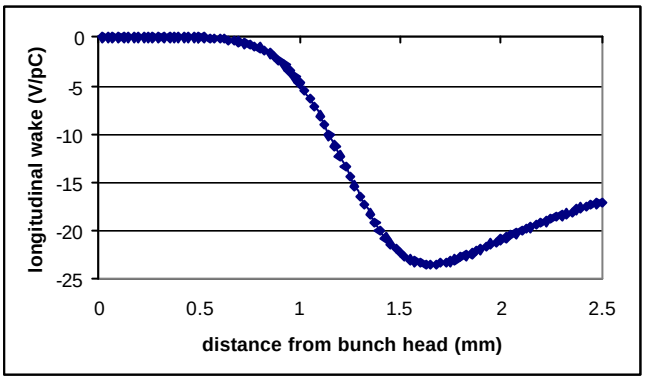

Figure 5: Longitudinal wakefield of one cavity with 0.25-mm-long bunch derived from wake green function

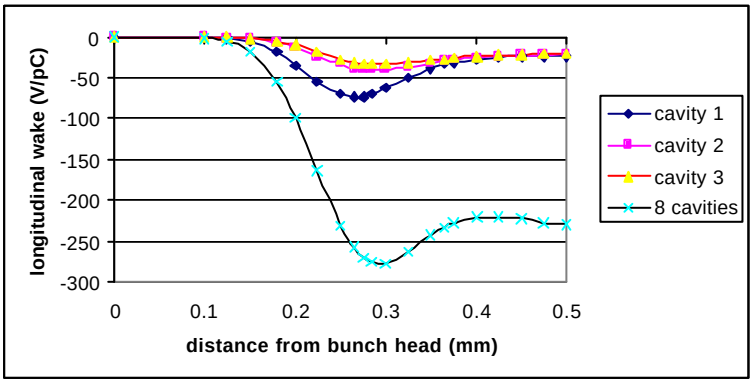

Figure 6: Longitudinal wakefield of the first 3 cavities and total 8 cavities with the bunch length of 0.05 mm

d. Wakefield of 0.05 mm

Similar to the case of 0.25 mm, the wakefield of the first 3 cavities are calculated with numerical codes and the wakefield of other 5 cavities is also derived from the green function, as shown in Figure 6.

2.1.2 Bellows

The cavities are connected by short bellow sections to allow for length variations of the cavity and thermal contraction during cooling down. Consideration has been given to the installation of an RF shielding to avoid the HOM loss in the bellows which add to the cryogenic load at 1.8 K. However, all designs showed that this will take the danger of producing metallic dust by friction. Therefore, the RF shielding is not installed in the bellows in the TTF Linac [5]. There are several types of bellows in the TTF Linac with different number of waves and different beam pipe radius. In this section, the wakefield of bellow with 4 waves are calculated. The wakefield of other types bellows can then be simply scaled from it, since its wakefield is linear with the number of the waves and inverse to the square of the beam pipe radius. The schematic map of the bellow and its longitudinal wakefield with different bunch length are given in Figure 7 and 8, respectively.

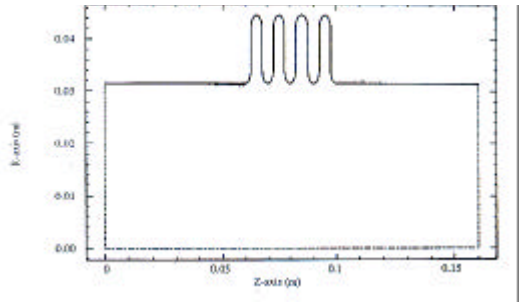

Figure 7: Schematic structure of bellow

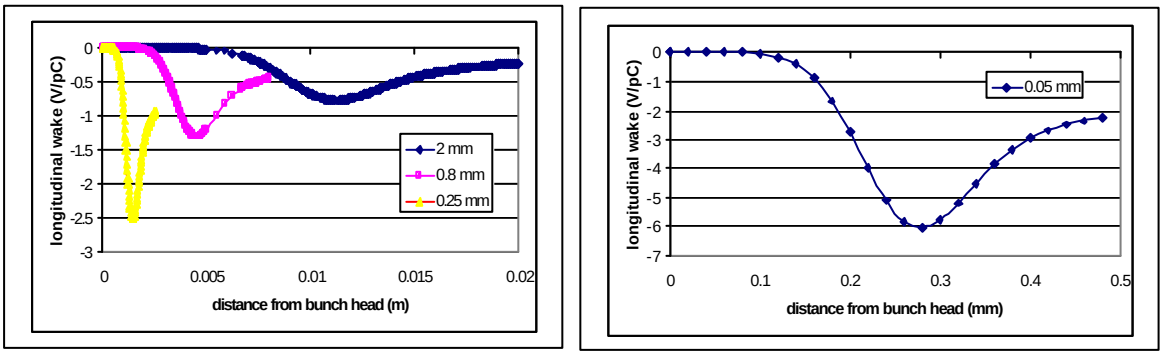

Figure 8: Longitudinal wakefield of bellow with different bunch length of 2 mm, 0.8 mm, 0.25 mm and 0.05 mm

2.1.3 Valves

The valves in the TTF Linac are used to isolate the vacuum in one section from the vacuum of adjacent section. Each module of 8 cavities has valves at either end. A valve in the beamline is like a rectangular cavity when it is open. The structure of the valve used in the calculation is simplified as shown in Figure 9 with a square cross-section and a gap of 25 mm [6]. In the calculations, the square cross section of the outer valve pipe can be considered as the circular one, since the corners contribute less to the wakefield. With 2-D ABCI code, the wakefield of a valve with different bunch length is shown in Figure 10.

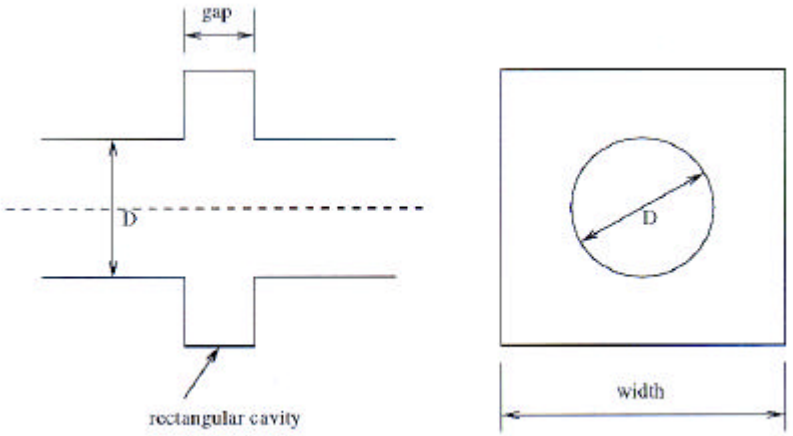

Figure 9: Schematic map of the gate valve structure

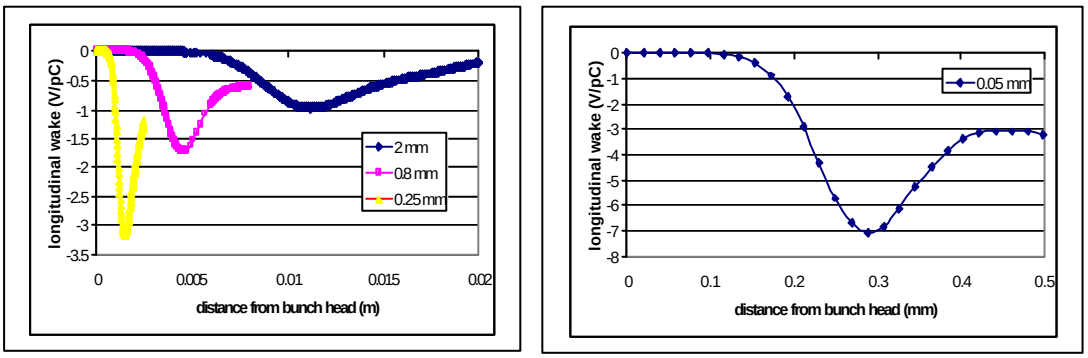

(a) (b)

Figure 10: Longitudinal wakefield of the gate valve with the bunch length of 2 mm, 0.8 mm, 0.25 mm and 0.05 mm

2.1.4 Others

The wakefield of resistive wall, BPMs, flanges and other components are not addressed in this section, since their contribution is smaller and could be neglected.

2.2 Correlated energy spread

The longitudinal wake fields can affect the energy distribution of the particles in one bunch. The change of energy distribution after one accelerating structure can be given by:

$$\Delta E(s) = G_{acc} L \cdot \cos(j_0 + 2pf_0 s/c) + NeW_{11}(s) \quad (4)$$

where G_{acc} the accelerating gradient of the structure, L the structure length, j_0 the initial RF phase, f_0 the RF frequency, N the particle number in the bunch, W_{11}(s) the longitudinal wakefield. The correlated energy spread due to longitudinal wakefield is [3]:

$$dE = qe\sqrt{\int ds \cdot r(s) \cdot W_{11}^{\ 2}(s) - k_{11}^{\ 2}} \quad (5)$$

where k_{11} is the loss factor,

$$k_{11} = \int ds \cdot r(s) \cdot W_{11}(s) \quad (6)$$

In the 8-cavity wakefield calculation for the short bunch length, the wakefield of the cavity from #4 to #8 are derived from the wake green function, as considered in the last section. The energy spread induced by the wakefield of cavity #3 and #8 has been compared, as listed in Table 2. It is shown that the difference of both energy spreads could be neglected.

Table 2: Energy spread comparison (unit: keV)

	Cavity #3	Cavity #8
s_z = 0.25 mm	7.4	7.2
s_z = 0.05 mm	9.6	9.2

The loss factors and correlated energy spread in the TTF FEL phase I and II are summarized in Table 3.

Table 3: The loss factor and its related broadening energy spread

Phase I	k_{11} (V/pC)	dE (keV)
Capture cavity (2 mm)	8.3	3.7
RF module 1 (0.8 mm)	86.63	40
RF module 2 and 3 (0.25 mm)	113.4*2	58.4
Bellows (2 mm)	6.0	3
Bellows (0.8 mm)	42.6	21.3
Bellows (0.25 mm)	80	40
Valves (2 mm)	2.75	1.4
Valves (0.8 mm)	3.72	1.86
Valves (0.25 mm)	13.3	6.63
Total	470.1	176.3
Relative energy spread	0.05% (380 MeV)	

Phase II	k_{11} (V/pC)	dE (keV)
Capture cavity (2 mm) RF module 1 (0.8 mm)	8.3 86.63	3.7 40
RF module 2 and 3 (0.25 mm)	113.4*2	58.4
RF module 4, 5, 6, 7 and 8	198.5*5	400
Bellows (2 mm)	6.0	3
Bellows (0.8 mm)	42.6	21.3
Bellows (0.25 mm)	80	40
Bellows (0.05 mm)	404	202
Valves (2 mm)	2.75	1.4
Valves (0.8 mm)	3.72	1.86
Valves (0.25 mm)	13.3	6.63
Valves (0.05 mm)	40	20
Total	1906.6	798.3 (keV)
Relative energy spread	0.08% (1.0 GeV)	

3 Transverse wakefield and its induced emittance growth for the single bunch

3.1 Transverse wakefield

Transverse (dipole) wakefields are excited if the beam traverses an accelerating structure off axis. The fields excited by the head of the bunch will kick the tails of the bunch even more off axis. The whole bunch may develop a banana shape tail, as shown in Figure 11. This can strongly dilute the emittance of the beam.

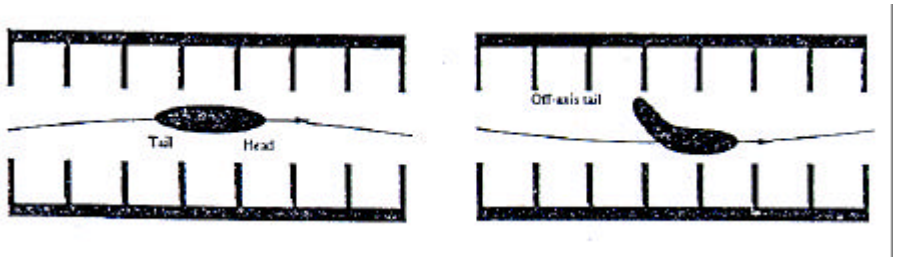

Figure 11: Banana shape of a bunch with off axis in the structures

The dipole wakefield is related with the bunch length as follows:

$$W_{\perp} \propto \frac{\sqrt{s_z}}{a^3} \tag{7}$$

where a is the radius of the beam pipe, s_z is the bunch length. Therefore, the shorter the bunch, the smaller the transverse wakefield. For the TTF Linac, we can give its upper

estimation of the emittance growth for one cavity offset with 2-mm-long bunch transverse wakefield. The transverse wake green function of one TESLA cavity is fitted as [7]:

$$W^{d}{}_{\perp}(s) = 1290\sqrt{s} - 2600s \ \text{(V/pC/m)} \tag{8}$$

where s is the distance from point charge. Using the relation between the transverse wakefield of the bunch and point charge:

$$W_{\perp}(s) = \int r(s') \cdot W^{d}{}_{\perp}(s - s') \cdot ds', \tag{9}$$

the transverse wakefield of 2-mm-long bunch can be derived, as shown in Figure 12, which also agrees well with MAFIA calculations.

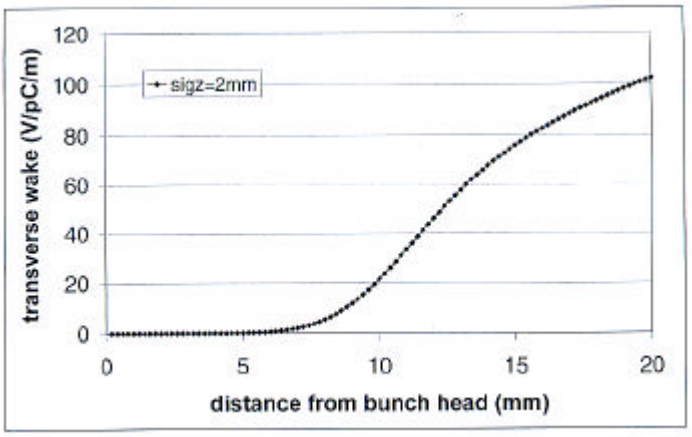

Figure 12: Transverse wakefield of one cavity
with the bunch length of 2 mm

3.2 Emittance growth

The differential equation of the transverse motion of a bunch with zero transverse dimension is given by:

$$\frac{d}{ds}\left(g(s)\frac{d}{ds}x(z,s)\right) + \left(\frac{2p}{l(s)}\right)^{2} g(s).x(z,s)$$
$$= \frac{1}{m_0 c^2} e^2 N_e \int_z^{\infty} r(z') W_{\perp}{}^{d}(z' - z, s).x(z', s)dz', \tag{10}$$

where $l(s)$ is the instantaneous wavelength of betatron focusing at position s, $g(s)$ is the normalized energy, N_e is the number of particles in bunch, $W^{d}{}_{\perp}(z)$ is the transverse wake green function per unit length in unit of V/pC/m. With the analogy to the Brownian

motion of a molecule, the emittance growth due to the transverse wakefield is expressed as [8]:

$$g\Delta e_x = \frac{< x >^2 L \cdot < b >}{2g(0)G_f}\left(\frac{e^2 N_e W_\perp(z)}{m_0 c^2}\right)^2 \qquad (11)$$

where $g\Delta e_x$ is the normalized transverse emittance, $< x >$ is the accelerating structure transverse offset in unit of meter, L is the structure length (m), $< b >$ is the betatron function (m), $g(0)$ is the normalized initial energy, $W_\perp(z)$ is the transverse wakefield per unit length at the tail of the bunch, usually at $2s_z$ in unit of V/pC/m/m, and G_f is given by:

$$g(s) = g(0) \cdot (1 + G_f \cdot s) \qquad (12)$$

where s is the total length of accelerating structures. In the TTF Linac, the beam is accelerated from the initial energy 5 MeV to the final 1 GeV with the accelerating gradient of 15 MV/m. The accelerating length of one cavity is 1 m, and the average beta function,

$$< b > = \frac{b_f + b_d}{2} \approx 10 \text{ m}, \qquad (13)$$

where b_f, b_d are the beta function at the focusing and defocusing quadrupoles, respectively. Substituting these parameters into Equation (11), the emittance growth induced by the transverse wakefield is given as:

$$g\Delta e_x = 2.75 \times 10^{-3} < x >^2 \text{ (m.rad)} \qquad (14)$$

In the usual case, there are two sources of offset between the beam and the axis of the accelerating structures. One is from the accelerating structure misalignments, and the other is from the beam jitter or beam offset, e.g., kick by the focusing solenoid which has a transverse offset in the RF gun [9]. In addition to the cavity misalignments, a transverse beam offset at the cavity entrance of 1 mm has been considered. Its wakefield induced emittance growth is calculated as shown in Table 4, which agrees well with simulation data [1].

Table 4: Emittance growth due to RF cavity misalignments

Rms cavity offset (mm)	Emittance growth
0.5	0.6%
0.8	0.9%
1	1.2%

4 Dispersion Induced Emittance Growth

For simplicity we consider a longitudinal positions s with maximum dispersion ($h' = 0$). Its emittance can then be written as:

$$e = e_0 + \Delta e_{wf}(s) + \Delta e_{disp}(s)$$

where the second term in the right side of the equation is the wakefield induced emittance growth, and the third term is the dispersion induced emittance growth, which can be calculated as follow:

$$\Delta e_{disp} \approx \frac{h^2(s) \cdot d^2(s)}{< b >}$$

where h is the centroid dispersion, d is the energy spread, and $< b >$ is the beta-function. In the TTF FEL, since $d \approx 0.1\%$, $< b > \approx 10$ m, and the dispersion is very small, obviously the dispersion induced emittance growth can be neglected.

5 Summary

The short-term wakefield and its induced correlated energy spread and emittance growth have been estimated. The correlated energy spread of TTF Linac except undulators is below 0.1% and its transverse wakefield induced emittance growth is near 1.0%.

Acknowledgements

I would like to give my thanks to M.Dohlus for his reading the manuscript. Also I would like to thank J.Rossbach and K.Floettmann for their hospitality during his stay at DESY.

References

1) "A VUV Free Electron Laser at the TESLA Test Facility at DESY", TESLA-FEL 95-03, 1995.
2) J.Rossbach, "The VUV free electron laser based on the TESLA test facility at DESY", EPAC98, 1998.
3) M.Dohlus, et al., "Estimation of longitudinal wakefield effects in the TESLA-TTF FEL undulator beam pipe and diagnostic section", TESLA-FEL 98-02, 1998.
4) A.Novokhatski and A.Mosnier, "Wakefield dynamics in quasi periodic structures", EPAC98, 1998.
5) D.Edwards(ed.), "TESLA Test Facility Linac-design report", TESLA 95-01, 1995.
6) Ch.Tang, et al., wakefield in the beamlines of TTF injector 2, TESLA-97-11, 1998
7) R.Brinkmann, et al.(eds), "Conceptual design of a 500 GeV electron-positron linear collider with integrated X-ray laser facility", DESY 1997-048, 1997.
8) J.Gao, "Analytical treatment of the emittance growth in the main linac of future colliders", LAL-SERA-99-82.
9) F.Zhou, "Emittance studies for the TTF FEL photoinjector", TESLA-FEL 99-02, 1992.